CONTROL OF SALTWATER INTRUSION IN UNCONFINED COASTAL AQUIFERS USING VERTICAL CUTOFF WALL

Sobhy R. Emara[1], Asaad M. Armanuos[2], Tamer A. Gado[3] and Bakenaz A. Zeidan [4]

[1]Irrigation and Hydraulics Engineering Department, Faculty of Engineering, Tanta University, Egypt
E-mail: sobhy_emara39@f-eng.tanta.edu.eg
[2]Irrigation and Hydraulics Engineering Department, Faculty of Engineering, Tanta University, Egypt
E-mail: asaad.matter@f-eng.tanta.edu.eg
[3]Irrigation and Hydraulics Engineering Department, Faculty of Engineering, Tanta University, Egypt
E-mail: tamer.gado@f-eng.tanta.edu.eg
[4]Irrigation and Hydraulics Engineering Department, Faculty of Engineering, Tanta University, Egypt
E-mail: b.zeidan@f-eng.tanta.edu.eg
** Corresponding Author: asaad.matter@f-eng.tanta.edu.eg*

ABSTRACT

The degradation of coastal aquifers is a pervasive environmental issue globally, as rising demand for groundwater for human and agricultural consumption, coupled with climate change, has led to saltwater intrusion. The research utilized SEAWAT numerical modeling to investigate the effectiveness of vertical cutoff walls in mitigating saltwater intrusion in coastal aquifers. Three different aquifer configurations were explored, including two stratified aquifers with different patterns of high and low hydraulic conductivity values (HLH and LHL) and a homogeneous aquifer (H). The study also examined three different cutoff wall depth ratios, including 0.849, 0.698, and 0.547. The dimensionless cutoff wall depth is a ratio of the cutoff wall depth relative to the aquifer depth.
The results showed that the vertical cutoff wall was successful in mitigating the saltwater wedge across all examined scenarios. The length of the toe decreased by about 37.7% for the cutoff wall depth ratio of 0.698 and by about 47% for the cutoff wall depth ratio of 0.849 in all investigated cases. These findings indicate that vertical cutoff walls can be an effective solution for preventing saltwater intrusion in coastal aquifers with different patterns of hydraulic conductivity values.

Keywords: Coastal Aquifers, Heterogeneous Aquifers, Cutoff Wall, Seawater Intrusion

1 INTRODUCTION

Coastal areas around the world are facing a serious issue known as seawater intrusion (SWI), which occurs when saline water from the sea contaminates the groundwater supply. This is especially problematic in regions where groundwater is the primary source of freshwater. Overuse of groundwater is a leading cause of SWI, rendering the contaminated water unsuitable for human consumption, agriculture, and industry. To combat this problem, underground physical barriers are effective solutions that store fresh groundwater supplies. The two most common types of underground barriers are the subsurface dam, which is constructed at the bottom of the aquifer with an opening at the top to allow for natural freshwater flow to the sea, and the cutoff wall, which physically restricts the movement of saline water toward land. Many studies have examined the effectiveness of these techniques in managing SWI, including works by (Senthilkumar and Elango, 2011; Abdoulhalik and Ahmed, 2017; Armanuos, 2017; Robinson et al., 2018).

Kaleris and Ziogas (2013) utilized SUTRA code to simulate the impact of using cutoff walls on the process of seawater intrusion and evaluate the protective impact on groundwater extraction close to the coastal region. The findings of this research revealed that without groundwater abstraction, the impact of using cutoff walls can be influenced by the depth of cutoff wall, the distance from the shoreline to the cutoff wall, the ratio of groundwater velocity, the mixing intensity, and the comparative conductivity of the cutoff wall. Figures and empirical formulas were displayed. The

maximum rate of safe abstraction before and after the wall construction was determined. The outcomes confirmed that the protective impact of the wall is strong in case of locating the wall close to the coast, with high relative wall depths, aquifer system with low velocity, low mixing and higher value of anisotropy.

Chang et al. (2022) used interior tests and simulation results to study the downstream seawater responses in the presence of cutoff walls. The findings demonstrated that cutoff walls would allow the downstream seawater wedge to increase, expand the mixing zone width, reduce freshwater outflow, and exacerbate beachside groundwater degradation in coastal groundwater aquifers. As a result, cutoff walls are not appropriate for coastal groundwater aquifers with minimal hydraulic gradients. The cutoff wall stays efficient for SWI management as the distance in between wall and the sea border decreases. As a result, we discovered that a cutoff wall nearer to the sea could reduce groundwater salt accumulation in coastal groundwater aquifers without raising building costs.

Zheng et al. (2020) suggested a new variable-perviousness cut-off wall featuring a semi-pervious portion at the bottom of the physical barrier. This is the only research to look at the spatial spreading and transient behaviors of SI and nitrate contamination at the field level. The findings shows that dissolved oxygen declines virtually simultaneously with the invasion of SW close to the sea border, and that denitrification of NO3 and retreating of the dissolved organic carbon wedge happened in the interior aquifer. Interestingly, the freshwater discharge flow and nitrate discharge flux increased by 35% and 20%, correspondingly, whereas the enriching ration of volume of nitrate contaminated region decreased by 15%.

Utilizing experimental and computer simulations studies, Abdoulhalik et al. (2022a) investigate the effect of cutoff walls on seawater upconing. The findings indicate that in the tested arrangements, the cutoff wall did not significantly postpone the saline upconing process. Cutoff walls' protective function was significantly susceptible to designing settings. Cutoff walls erected near to the pumped well, in particular, allowed the deployment of high discharge rate, resulting in a more efficient utilization freshwater, particularly for deeper wells. The findings revealed that the depth of penetration of the cutoff barriers does not always need to reach the depth of the pumping well to improve the performances, and it is critical from both a building and economic standpoint.

Li et al. (2018) used a sandbox experiment as a physical model and the FEFLOW model to compare the dynamics of seawater intrusion using and without underground barriers. The seawater front might still get past the subterranean barrier and keep going forward, according to the findings. These findings revealed that underground barriers with limited permeability could successfully avoid seawater intrusion. The findings of this research study have significant practical implications for the avoidance of seawater intrusion in coastal locations.

Armanuos et al. (2019) conducted experimental and numerical experiments to assess the impact of utilizing cutoff wall, a recharge well, or a combine of these to mitigate SWI. The SEAWAT model was employed to simulate the SWI wedge and the dynamics of the retreated remaining seawater just after remedial procedures were implemented. The combining of flow barrier and freshwater injection pushed the seawater to recede, resulting in repulsion ratio values higher than the cutoff wall or freshwater injection alone.

Zheng et al. (2021)Zheng et al. (2021) investigated the best position of cutoff walls for saltwater intrusion using the simulation-optimization approach. The placement of the cutoff wall that reduces the total of the chlorine concentrations in the two freshwater resources is established. This technology offers a strong and dependable way for locating cutoff walls for upcoming work aimed at preventing and controlling saltwater intrusion.

Zheng et al. (2022) used both numerical and experimental analysis to investigate the dynamic behavior and desalination mechanism of invading saltwater following the installation of a cut-off wall. The simulation results indicate that a quick seawater retreading process is happening in a short amount of time, whereas the retreating of the remaining seawater wedge is gradual at first. The

quantity of remaining seawater is mostly determined by the depths and the hydraulic conductivity of the cut-off wall, whereas the retreating period is influenced by the wall's position. However, a deeper cut-off wall can improve remaining seawater removal.

Previous studies on controlling SWI mostly used homogeneous mediums, which do not reflect real-world conditions where site heterogeneity is common and increasingly prevalent (Abdoulhalik and Ahmed, 2017).

Abd-Elaty et al. (2019) investigated the use of physical underground barriers (PSB) to control SWI in the Biscayne aquifer, USA. Various scenarios of barrier penetration depths, positions, and permeability have indeed been investigated. The findings demonstrate that the PSB can successfully limit saltwater intrusion. Cutoff walls, on the other hand, provided greater repulsion than underground dams.

The primary goals of this study are twofold:

(1) to investigate how effective vertical physical barriers are in controlling SWI in heterogeneous soil formations, thereby enabling a more realistic assessment of their performance; and

(2) to clarify the timeframes and dynamic behaviors of removing residual saltwater at different aquifer features and different cutoff wall depths, using removal efficiency as an indicator of cutoff wall effectiveness (Luyun Jr et al., 2009; Zheng et al., 2019).

2 METHODOLOGY

The numerical simulation model for solute transport in groundwater flow was constructed using SEAWAT, which is commonly employed for simulating variable-density flow in groundwater (Guo and Langevin, 2002).

The numerical simulation model of solute transport in groundwater flow is constructed using SEAWAT, which has been widely used to simulate groundwater variable-density flow (VDF) based on the finite-difference groundwater flow simulation model MODFLOW (Guo and Langevin, 2002). The flux equation and the transport equation used in the SEAWAT were shown in Equations (1) and (2), respectively:

$$\frac{\partial}{\partial\alpha}\left(\rho k_{f\alpha}\left[\frac{\partial h_f}{\partial\alpha}+\frac{\rho-\rho_f}{\rho_f}\frac{\partial Z}{\partial\alpha}\right]\right)+\frac{\partial}{\partial\beta}\left(\rho k_{f\beta}\left[\frac{\partial h_f}{\partial\beta}+\frac{\rho-\rho_f}{\rho_f}\frac{\partial Z}{\partial\beta}\right]\right) + \frac{\partial}{\partial\gamma}\left(\rho k_{f\gamma}\left[\frac{\partial h_f}{\partial\gamma}+\frac{\rho-\rho_f}{\rho_f}\frac{\partial Z}{\partial\gamma}\right]\right)=\rho S_f\frac{\partial h_f}{\partial t}+\theta\frac{\partial\rho}{\partial C}\frac{\partial C}{\partial t}-\rho_S q_S \quad (1)$$

where α, β, and γ is the groundwater flow direction; $k_{f\alpha}$, $k_{f\beta}$ and $k_{f\gamma}$ are the hydraulic conductivity of groundwater flow in different directions, respectively; S_f is the specific storage in terms of the freshwater head; θ is the effective porosity; ρ is the density of saline groundwater at a point in the aquifer; ρ_f is the density of freshwater; ρ_S and q_S denote the density and volume of the dissolved substance at the source and sink terms, respectively.

$$\frac{\partial(\theta C^k)}{\partial t}=\frac{\partial}{\partial x_i}\left(\theta D_{ij}\frac{\partial C^k}{\partial x_j}\right)-\frac{\partial}{\partial x}\left(\theta V_i C^k\right)+q_S C_k^S+\sum R_n \quad (2)$$

where C^k represents the concentration of the solute substance; C is the solute concentration of the substance in the source and sink term; $\sum R_n$ represents the reaction term of the chemical substance in the aquifer; D the hydrodynamic dispersion coefficient tensor.

In this study, the dimensions of the experimental unconfined aquifer used by Gao *et al.* (2021) were used to validate the numerical model. The SEAWAT simulation area consists of a two-dimensional vertical section with dimensions of 90.0 cm × 28.0 cm that has been equally discretized to a finite-difference grid with quadratic elements with sizes of Δx × Δz = 0.5 cm × 0.5 cm. By satisfying the Péclet number (Pe_m) criterion, the dispersivity and element size provided sufficient numerical stability (Voss and Souza, 1987). The criterion for the Péclet number is as follows:

$$Pe_m \approx \frac{\Delta x}{\alpha_l} = 3.33 < 4 \qquad (3)$$

where Δx is the grid size in the X direction and the α_l is the aquifer longitudinal dispersivity. Two sets of three different configurations were done in total, including one set of baseline cases and the second set incorporating the cutoff wall. The influence of MPB was investigated in three distinct aquifer settings, including a homogeneous case (case H) and two multi-layered aquifers (high K–low K–high K - case HLH and low K–high K–low K - case LHL) as shown in Figure 2.
A total of 12 simulation groups were performed. Figure 1 represents the Boundary conditions for the numerical simulations.

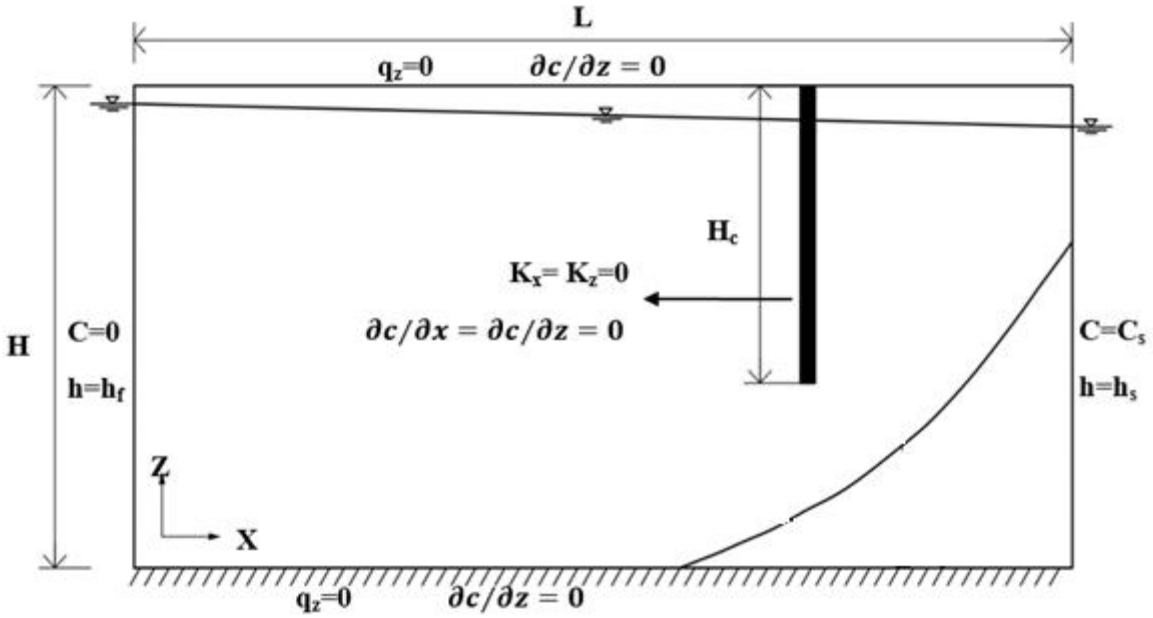

Figure 1 Boundary conditions for the numerical simulations. H and L are the height and length of the simulated domain. The cutoff wall depth is represented by H_c

The concentration was set to C_s = 36 g/L at the right-side saltwater boundary with a constant head of 26.5 cm (h_s). A hydraulic gradient of 0.0111 was applied to the system by adjusting the freshwater level to create head differences of 1.0 cm (h_f=27.5 cm). This value is within the range of gradients typically employed in prior laboratory scale research of a similar nature (Chang and Clement, 2012; Abdoulhalik and Ahmed, 2017; Abdoulhalik et al., 2022b). The freshwater concentration on the left side was fixed at C_f = 0 g/L. Freshwater and saltwater densities were 1000 kg/m^3 and 1025 kg/m^3, respectively. Figure 1 represents the Boundary and initial conditions for the numerical simulations.

Table 1. Summary of model parameters

Parameter	Value	Unit
Domain length (L)	90	cm
Domain height (H)	28	cm
Freshwater head (h_f)	27.5	cm
Saltwater head (h_s)	26.5	cm
Freshwater density (ρ_f)	1000	kg/m^3
Saltwater density (ρ_s)	1025	kg/m^3
Freshwater concentration (C_f)	0	mg/L
Saltwater concentration (C_s)	36000	mg/L
Investigated aquifer settings	case H; case HLH, case LHL	-
Hydraulic conductivity (K_H) High K layer	0.48	cm/s
Hydraulic conductivity (K_L) Low K layer	0.16	cm/s
Porosity (n)	0.4	-
Longitudinal dispersivity (α_L)	0.15	cm
Transversal dispersivity (α_T)	0.015	cm
Specific yield (S_y)	0.2	-
Cutoff wall depth (H_c)	16, 20, 24	cm
Dimensionless Cutoff wall depth ($H_c^* = 1 - \frac{H - H_c}{h_s}$)	0.547, 0.698, 0.849	-

Figure 2 represents a schematic design of the investigated aquifer settings in the study. There are three different aquifer configurations explored in the study, namely the homogeneous case (H), the HLH case, and the LHL case.

In the homogeneous case (H), the aquifer is uniform and has the same hydraulic conductivity throughout. In the HLH case, the aquifer consists of three layers, with a high hydraulic conductivity layer (L) located between two high hydraulic conductivity layers (H). This configuration leads to a high-low-high pattern of hydraulic conductivity. In the LHL case, the aquifer also consists of three layers, but the high hydraulic conductivity layer (H), located between two low hydraulic conductivity layers (L). This configuration leads to a low-high-low pattern of hydraulic conductivity.

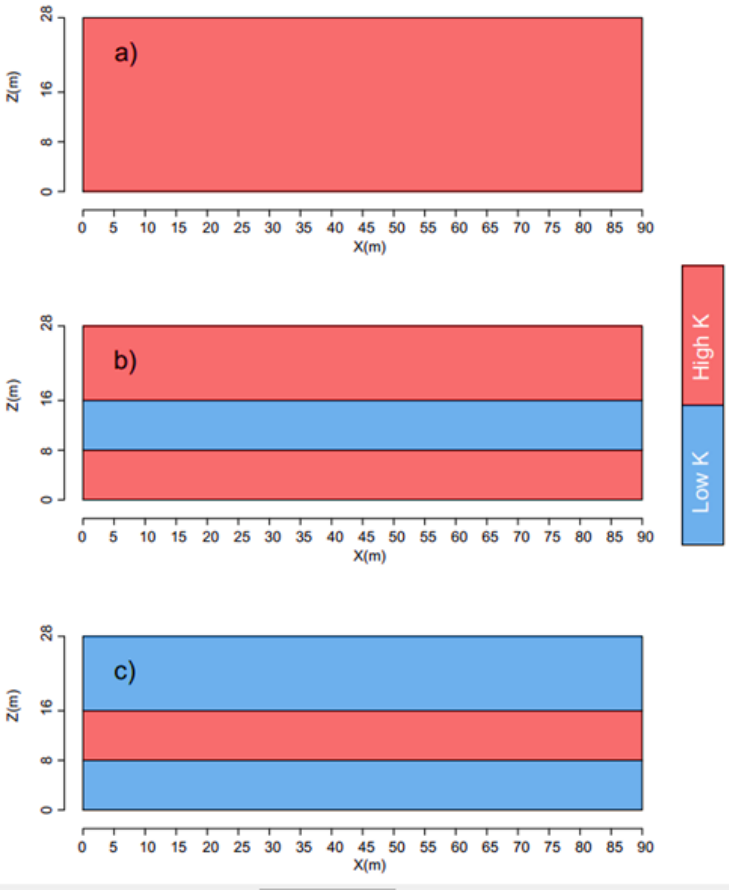

Figure 2 Schematic design of the investigated aquifer settings: a) homogeneous case H; b) case HLH and c) case LHL

3 RESULTS AND DISCUSSIONS

The length changes of the saltwater wedge from the experimentation carried out by Gao *et al.* (2021) were used to validation the numerical model in the case of homogenous configuration. Figure *3* demonstrates the agreement between the transient experimental and numerical results in the intrusion process in the baseline condition (homogenous configuration). Both the experiment and simulation performed well R^2 values of 0.9974.

The numerical model was validated for the homogeneous configuration using the length variations of the saltwater wedge observed in the experiments conducted by Gao et al. (2021) Figure *3* shows good agreement between the transient experimental and numerical results during the intrusion process in the baseline condition (homogeneous configuration), with both the experiment and simulation achieving high R^2 values of 0.9974.

The 50 percent seawater salinity isoline was identified in the model by visualizing the 18000 mg/L isoline.(Luyun Jr et al., 2011).

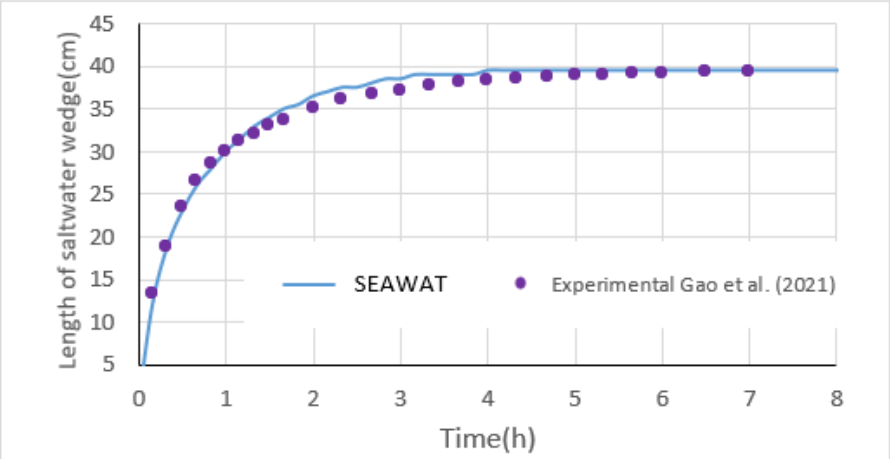

Figure 3 Comparison of the transient experimental after Gao et al. (2021) and numerical length of the saltwater wedge in the intrusion process

The impact of vertical cutoff wall for case H, case HLH, and case LHL is presented in Figure ***4***, , and Figure ***5*** , respectively. Figure ***6*** a, Figure ***4*** a, and Figure ***5*** a represent the steady state saltwater wedge before the installation of the vertical cutoff wall Figure ***6*** for case H, case HLH, and case LHL, respectively. b, Figure ***4*** b, and Figure ***5*** Figure ***6***b represent the steady state saltwater wedge after the installation of the vertical cutoff wall for case H, case HLH, and case LHL, respectively demonstrating the efficacy of vertical cutoff wall in saltwater removal from costal unconfined aquifers.

a)

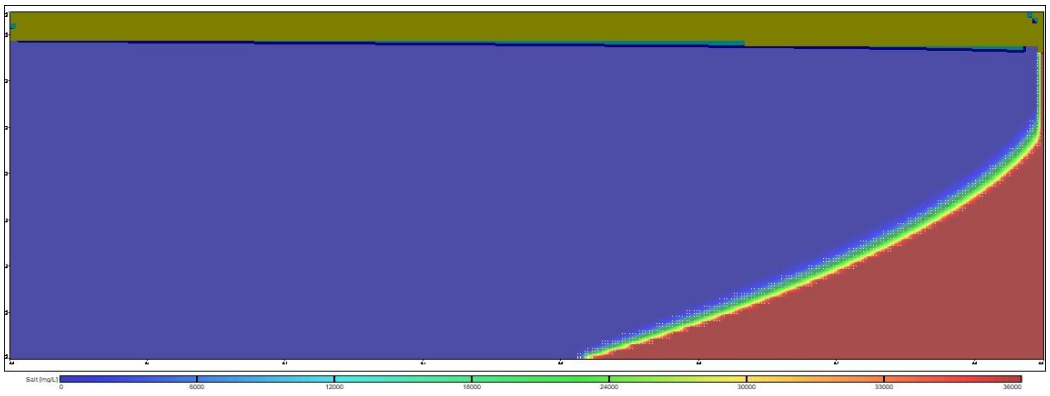

b)

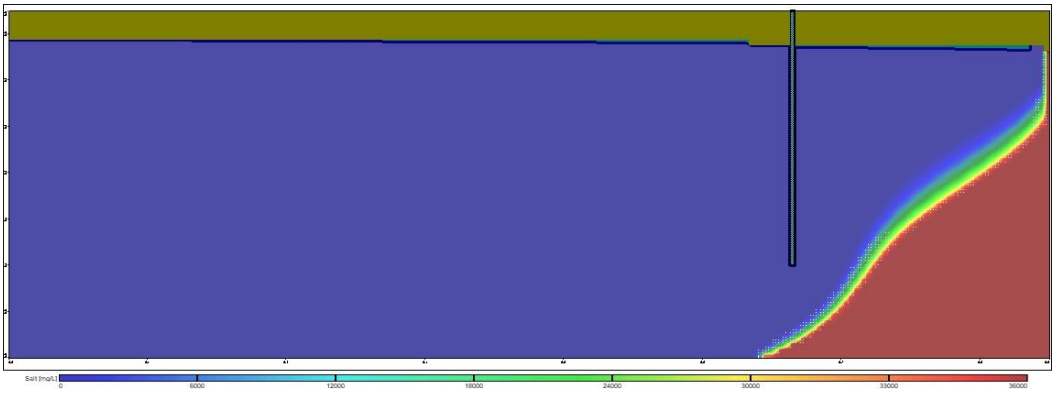

Figure 4 The steady state saltwater wedge for the homogeneous aquifer Case H a) Base case and b) cutoff wall depth equals 20cm (H_C*=0.698)

a)

b)

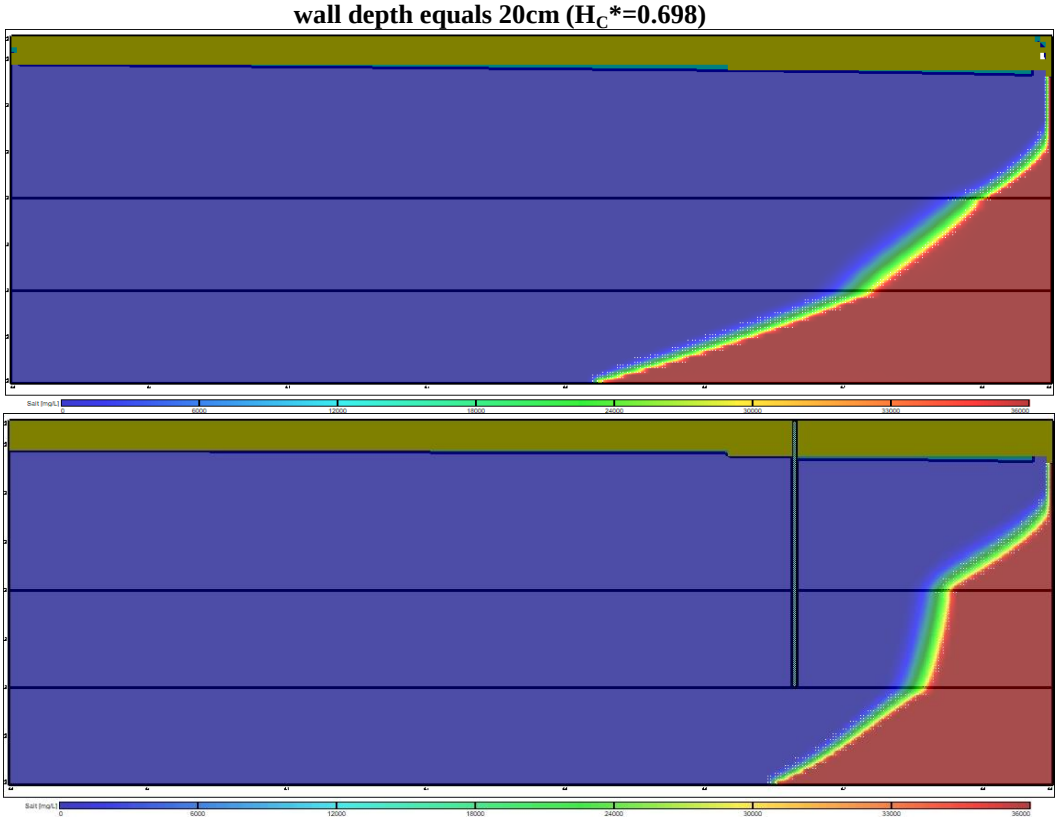

Figure 5 The steady state saltwater wedge for the layered aquifer Case HLH a) Base case and b) cutoff wall depth equals 20cm (H_C*=0.698)

a)

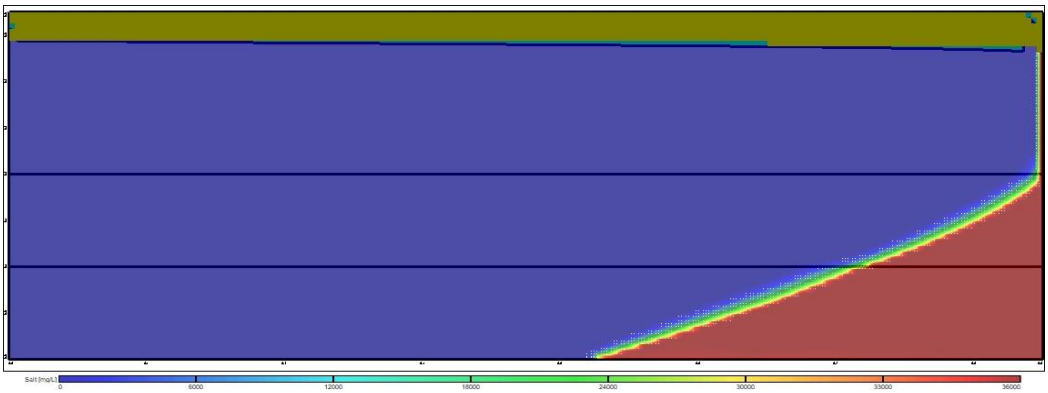

b)

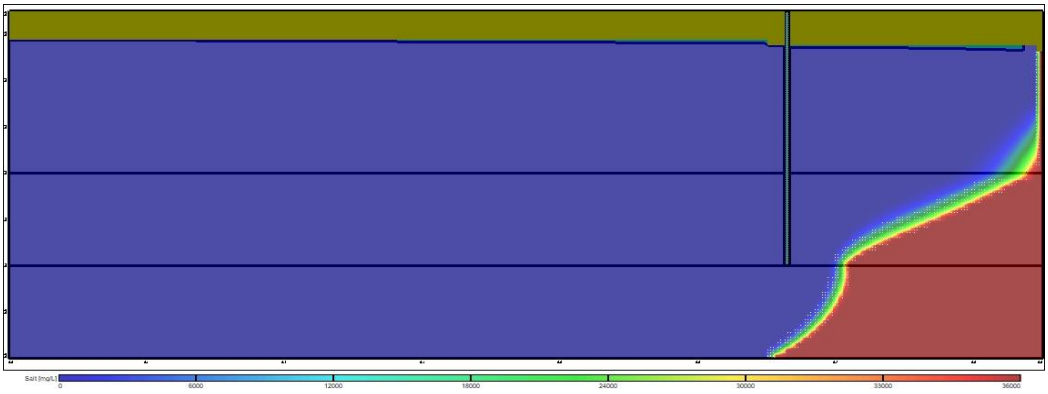

Figure 6 The steady state saltwater wedge for the layered aquifer Case LHL a) Base case and b) cutoff wall depth equals 20cm (H_C*=0.698)

The reduction rate of saltwater wedge length (R_L) was established to assess the removal effectiveness of saltwater intrusion after the construction of the vertical cutoff wall. The index was calculated as follows:

$$R_L = \frac{L_i - L}{L_i} \qquad (4)$$

where L_i is the saltwater wedge's initial length in baseline cases and L is the residual saltwater wedge's length after the cutoff wall installation. L_i and L are both defined as the distance between the saltwater boundary and the residual saltwater toe. The toe location was identified using a 50 % seawater salinity isoline (18000 mg/L).

To explore the effect of cutoff wall depth on removal efficiency, varied cutoff wall depth Hc values were used.

Figure *7* depicts the changes in R_L over time. However, a cost-benefit analysis is necessary to assess the feasibility and cost of building cutoff wall.

a)

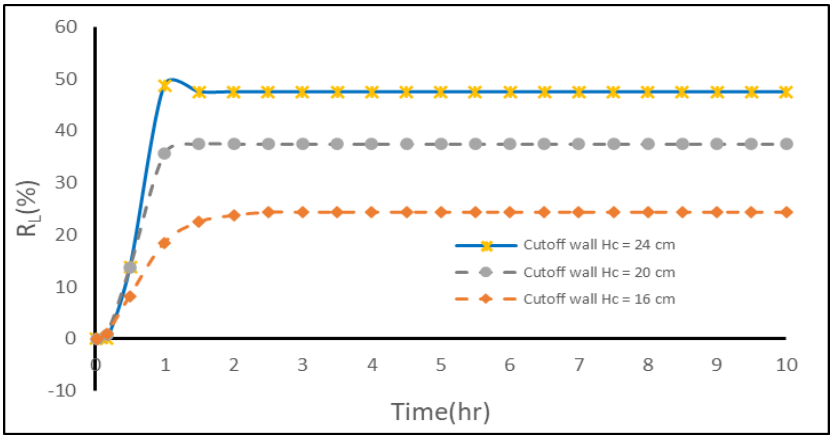

b)

c)

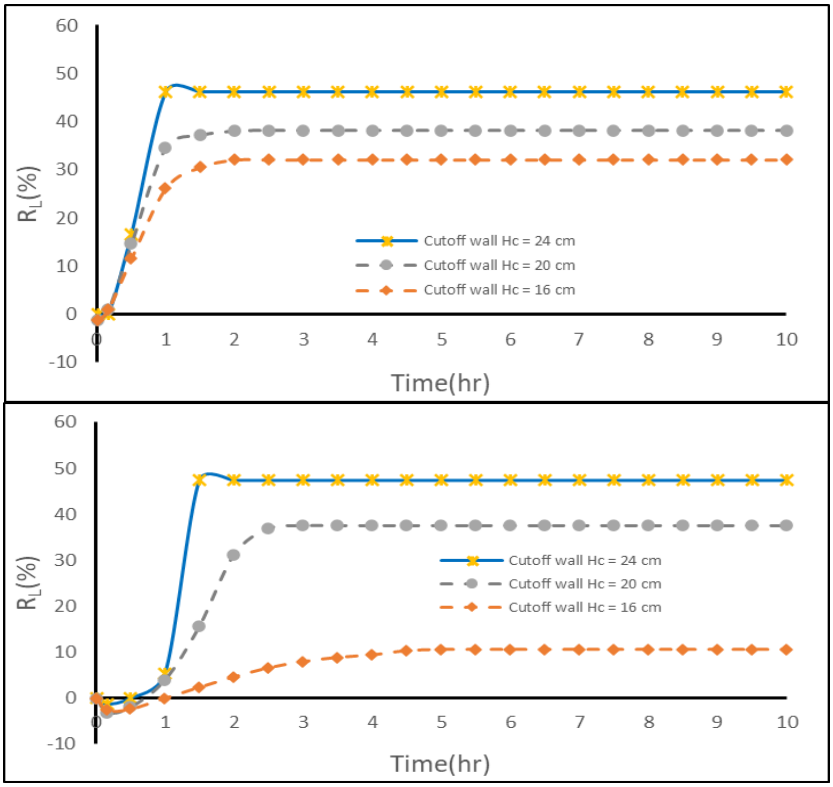

Figure 7 Influences of cutoff wall depth on saltwater removal reduction rate for a) Case H, b) Case HLH, and c) Case LHL

The vertical cutoff wall was successful in mitigating the saltwater wedge across all examined scenarios. In all the investigated cases, the length of the toe decreased by about 37.7% for the cutoff wall depth ratio of 0.698, and by about 47% for the cutoff wall depth ratio of 0.849 as shown in Figure 7.

The study determined that the amount of time it took for the saltwater wedge to reach a steady state varied based on the cutoff wall depth ratio and the configuration of the aquifer. Specifically, for the homogenous aquifer (case H), the saltwater wedge reached steady state after 1.5, 1.5, and 2.33 hours for cutoff wall depth ratios of 0.547, 0.698, and 0.849, respectively. For the HLH case, the saltwater wedge reached steady state after 1.0, 2.0, and 2.0 hours for cutoff wall depth ratios of 0.547, 0.698, and 0.849, respectively. Finally, for the LHL case, the saltwater wedge reached steady state after 1.5, 3.0, and 5.0 hours for cutoff wall depth ratios of 0.547, 0.698, and 0.849, respectively.

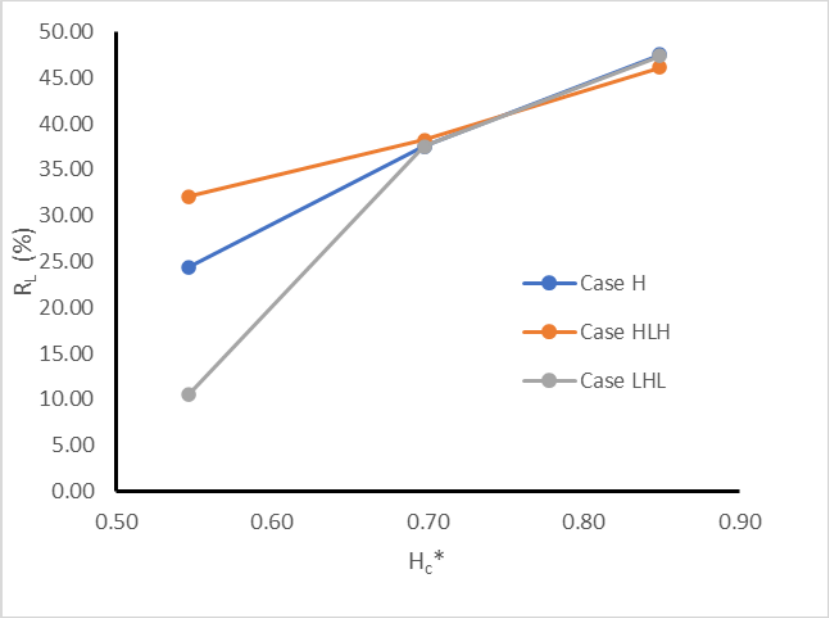

Figure 8 The repulsion ratio R_L verses dimensionless cutoff wall depth (H_c*)

CONCLUSIONS

The study utilized a validated numerical model, the SEAWAT model, to investigate the impacts of vertical cutoff walls on saltwater removal from unconfined multi-layered coastal aquifers. The SEAWAT model predicted the transient toe movement of the saltwater wedge relatively well in both the intrusion process, with R^2 values of 0.9974. The study found that the vertical cutoff wall effectively reduced the intrusion of saltwater into groundwater aquifers in all scenarios examined. The length of the toe, which represents the extent of saltwater intrusion, was reduced by approximately 37.7% and 47% when the cutoff wall depth ratios were 0.698 and 0.849, respectively.

These findings indicate that the cutoff wall effectively blocked the movement of saltwater and prevented it from contaminating the fresh water in the aquifer. The study provides valuable insights for the management and protection of coastal aquifers, especially in areas where saltwater intrusion is a major concern. The study contributes to the understanding of the effectiveness of vertical cutoff walls in preventing saltwater intrusion in coastal aquifers. Nonetheless, a cost-benefit analysis is necessary to assess the feasibility and cost of building cutoff wall.

REFERENCES

Abdoulhalik, A., Abdelgawad, A.M., Ahmed, A.A., Moutari, S., Hamill, G., 2022a. Assessing the protective effect of cutoff walls on groundwater pumping against saltwater upconing in coastal aquifers. Journal of Environmental Management 323, 116200. https://doi.org/10.1016/j.jenvman.2022.116200

Abdoulhalik, A., Ahmed, A., Abdelgawad, A., Hamill, G., 2022b. The impact of a low-permeability upper layer on transient seawater intrusion in coastal aquifers. Journal of Environmental Management 307, 114602. https://doi.org/10.1016/j.jenvman.2022.114602

Abdoulhalik, A., Ahmed, A.A., 2017. The effectiveness of cutoff walls to control saltwater intrusion in multi-layered coastal aquifers: Experimental and numerical study. Journal of Environmental Management 199, 62–73. https://doi.org/10.1016/j.jenvman.2017.05.040

Armanuos, A.M., 2017. Experimental and numerical study of saltwater intrusion in the Nile delta aquifer, Egypt (PhD Thesis). Egypt-Japan University of Science and Technology (E-JUST).

Armanuos, A.M., Ibrahim, M.G., Mahmod, W.E., Takemura, J., Yoshimura, C., 2019. Analysing the Combined Effect of Barrier Wall and Freshwater Injection Countermeasures on Controlling Saltwater Intrusion in Unconfined Coastal Aquifer Systems. Water Resour Manage 33, 1265–1280. https://doi.org/10.1007/s11269-019-2184-9

Chang, Q., Zheng, T., Gao, C., Zheng, X., Walther, M., 2022. How to cope with downstream groundwater deterioration induced by cutoff walls in coastal aquifers. Journal of Hydrology 610, 127804. https://doi.org/10.1016/j.jhydrol.2022.127804

Chang, S.W., Clement, T.P., 2012. Experimental and numerical investigation of saltwater intrusion dynamics in flux-controlled groundwater systems. Water Resources Research 48. https://doi.org/10.1029/2012WR012134

Gao, M., Zheng, T., Chang, Q., Zheng, X., Walther, M., 2021. Effects of mixed physical barrier on residual saltwater removal and groundwater discharge in coastal aquifers. Hydrological Processes 35. https://doi.org/10.1002/hyp.14263

Guo, W., Langevin, C.D., 2002. User's guide to SEAWAT; a computer program for simulation of three-dimensional variable-density ground-water flow.

Kaleris, V.K., Ziogas, A.I., 2013. The effect of cutoff walls on saltwater intrusion and groundwater extraction in coastal aquifers. Journal of Hydrology 476, 370–383. https://doi.org/10.1016/j.jhydrol.2012.11.007

Li, F., Chen, X., Liu, C., Lian, Y., He, L., 2018. Laboratory tests and numerical simulations on the impact of subsurface barriers to saltwater intrusion. Nat Hazards 91, 1223–1235. https://doi.org/10.1007/s11069-018-3176-4

Luyun Jr, R., Momii, K., Nakagawa, K., 2011. Effects of recharge wells and flow barriers on seawater intrusion. Groundwater 49, 239–249.

Robinson, G., Moutari, S., Ahmed, A.A., Hamill, G.A., 2018. An Advanced Calibration Method for Image Analysis in Laboratory-Scale Seawater Intrusion Problems. Water Resour Manage 32, 3087–3102. https://doi.org/10.1007/s11269-018-1977-6

Senthilkumar, M., Elango, L., 2011. Modelling the impact of a subsurface barrier on groundwater flow in the lower Palar River basin, southern India. Hydrogeol J 19, 917. https://doi.org/10.1007/s10040-011-0735-0

Voss, C.I., Souza, W.R., 1987. Variable density flow and solute transport simulation of regional aquifers containing a narrow freshwater-saltwater transition zone. Water Resources Research 23, 1851–1866. https://doi.org/10.1029/WR023i010p01851

Zheng, H., Wenxi, L., Yue, F., Tiansheng, M., Jin, L., Jiuhui, L., 2021. Optimal location of cutoff walls for seawater intrusion. Appl Water Sci 11, 179. https://doi.org/10.1007/s13201-021-01514-1

Zheng, T., Gao, M., Chang, Q., Zheng, X., Walther, M., 2022. Dynamic Desalination of Intruding Seawater After Construction of Cut-Off Walls in a Coastal Unconfined Aquifer. Frontiers in Marine Science 9.

Zheng, T., Zheng, X., Sun, Q., Wang, L., Walther, M., 2020. Insights of variable permeability full-section wall for enhanced control of seawater intrusion and nitrate contamination in unconfined aquifers. Journal of Hydrology 586, 124831. https://doi.org/10.1016/j.jhydrol.2020.124831